Geomorphology 141-142 (2012) 88–98

Contents lists available at SciVerse ScienceDirect

Geomorphology

journal homepage: www.elsevier.com/locate/geomorph

Evidence for earthquake triggering of large landslides in coastal Oregon, USA

William H. Schulz [a,*], Sarah L. Galloway [a,1], Jerry D. Higgins [b,2]

[a] U.S. Geological Survey, Box 25046, MS-966, Denver, CO 80225, USA
[b] Colorado School of Mines, Dept. of Geology and Geological Engineering, Golden, CO 80401, USA

ARTICLE INFO

Article history:
Received 2 September 2011
Received in revised form 9 December 2011
Accepted 12 December 2011
Available online 19 December 2011

Keywords:
Landslide
Earthquake
Coastal bluff
Oregon
Tsunami
Cascadia subduction zone

ABSTRACT

Landslides are ubiquitous along the Oregon coast. Many are large, deep slides in sedimentary rock and are dormant or active only during the rainy season. Morphology, observed movement rates, and total movement suggest that many are at least several hundreds of years old. The offshore Cascadia subduction zone produces great earthquakes every 300–500 years that generate tsunami that inundate the coast within minutes. Many slides and slide-prone areas underlie tsunami evacuation and emergency response routes. We evaluated the likelihood of existing and future large rockslides being triggered by pore-water pressure increase or earthquake-induced ground motion using field observations and modeling of three typical slides. Monitoring for 2–9 years indicated that the rockslides reactivate when pore pressures exceed readily identifiable levels. Measurements of total movement and observed movement rates suggest that two of the rockslides are 296–336 years old (the third could not be dated). The most recent great Cascadia earthquake was M 9.0 and occurred during January 1700, while regional climatological conditions have been stable for at least the past 600 years. Hence, the estimated ages of the slides support earthquake ground motion as their triggering mechanism. Limit-equilibrium slope-stability modeling suggests that increased pore-water pressures could not trigger formation of the observed slides, even when accompanied by progressive strength loss. Modeling suggests that ground accelerations comparable to those recorded at geologically similar sites during the M 9.0, 11 March 2011 Japan Trench subduction-zone earthquake would trigger formation of the rockslides. Displacement modeling following the Newmark approach suggests that the rockslides would move only centimeters upon coseismic formation; however, coseismic reactivation of existing rockslides would involve meters of displacement. Our findings provide better understanding of the dynamic coastal bluff environment and hazards from future subduction-zone earthquakes.

Published by Elsevier B.V.

1. Introduction

Many large, deep, sporadically active or dormant rockslides occur along the Pacific coastline of Oregon (North and Byrne, 1965; Burns et al., 2011). Renewed, primarily slow movement (generally centimeters/week) of the sporadically active slides occurs during most rainy seasons following prolonged, intense rainfall (e.g., Schlicker et al., 1973). Their slow movement keeps pace with coastal bluff retreat; hence, their observed effects on coastal geomorphology are largely limited to progressive disruption of the marine terrace they occupy. The slides do not generally present extreme hazard to human safety because they move slowly; but they do destroy roadways, infrastructure, and homes and render U.S. Highway 101 (the Pacific Coast Highway) unusable at times causing economic hardship to coastal communities that rely on tourism for financial support. Although these rockslides are relatively innocuous compared to more rapidly moving slides, their potential reactivation and initiation of similar rockslides during a future earthquake could create significant hazards to human safety. Great earthquakes along the Cascadia subduction zone located offshore will occur in the future and cause considerable ground shaking that destroys buildings and infrastructure (Heaton and Hartzell, 1987; Clague, 1997). Paleoseismic studies suggest that these earthquakes recur every 300–500 years (e.g., Atwater and Hemphill-Haley, 1997; Kelsey et al., 2002, 2005; Nelson et al., 2004) and the last such earthquake occurred on 26 January 1700 with an estimated magnitude of 9.0 (Satake et al., 1996). Subduction-zone earthquakes may generate large tsunami that will reach the coastline within tens of minutes and cause widespread devastation (Priest, 1995), similar to the recent tragic illustrations from the great 2011 Japan and 2004 Sumatra earthquakes; the 1700 earthquake off the Oregon coast produced a tsunami that inundated coastal areas as high as 10–12 m above mean sea level (amsl) (Goldfinger et al., 2003; Geist, 2005). Coastal rockslides may experience substantial renewed movement during an earthquake and new rockslides may form. These rockslides may render tsunami evacuation and

* Corresponding author. Tel.: +1 303 273 8404; fax: +1 303 273 8600.
E-mail addresses: wschulz@usgs.gov (W.H. Schulz), gallowaysl@pbworld.com (S.L. Galloway), jhiggins@mines.edu (J.D. Higgins).
[1] Tel.: +1 970 270 6624; fax: +1 303 273 8600.
[2] Tel.: +1 303 273 3817; fax: +1 303 273 3859.

0169-555X/$ – see front matter. Published by Elsevier B.V.
doi:10.1016/j.geomorph.2011.12.026

emergency response routes unusable, potentially endangering the lives of many more people than currently anticipated.

To evaluate potential initiation mechanisms of large rockslides in coastal Oregon and seismogenic movement of existing slides, we studied three rockslides typical of the central coast (Fig. 1). Our studies included surface and subsurface characterization of the rockslides and monitoring of movement and hydrologic conditions related to their wet-season reactivation. Our results and inferred conditions at the time of rockslide formation were used in limit-equilibrium slope-stability analyses to evaluate potential initiation by increased pore-water pressures or earthquake ground shaking. Finally, we evaluated potential coseismic displacement of newly formed and reactivated rockslides following the Newmark (1965) approach. Our findings may be useful for regional hazard and risk assessments, as well as for increasing our understanding of processes that sculpt the dynamic coastal bluff environment in central Oregon. Additionally, the methods utilized herein could be useful for evaluating potential initiation mechanisms of other landslides. Jibson and Keefer (1993) demonstrated the utility of similar methods for evaluating potential triggering mechanisms for landslides in the New Madrid, USA seismic zone. Hence, these approaches also may be followed to estimate the relative contribution of earthquake-triggered landsliding to geomorphic evolution at multiple temporal and spatial scales.

2. Geologic setting

The Oregon coastal region (Fig. 1) is located upon the North American tectonic plate about 90 km east from where it overrides the Juan de Fuca plate forming the Cascadia subduction zone offshore (e.g., Clague, 1997). The rockslides we studied (Carmel Knoll, Devils Punchbowl, and Johnson Creek) occur mostly in carbonaceous and micaceous mudstone, siltstone, and sandstone of the middle Miocene Astoria Formation (North and Byrne, 1965; Schlicker et al., 1973; Priest and Allan, 2004), which has an approximate shear-wave velocity (V_s) of 613 m/s (Madin and Wang, 1999). Along the coast, the Astoria Formation strikes about north–south and dips ~10–30° west; however, the unit is mostly massive with poorly defined bedding and stratigraphic facies variation in the vicinity of the rockslides, being comprised mostly of clayey, sandy siltstone. Rugged basalt headlands also occur along the coastline; their much greater resistance to wave erosion relative to the sedimentary units has resulted in formation of numerous embayments typically several kilometers in along-shore length. The sedimentary rock units are uplifted and their upper surfaces are generally nearly flat, having been eroded into a series of marine terraces (Schlicker et al., 1973). Flat-lying Quaternary marine terrace sands generally a few meters thick cap most of the rock, forming a relatively flat ground surface that typically slopes only about 1° toward the coastline. These terrace sands can be very similar to parts of the Astoria Formation (Schlicker et al., 1973).

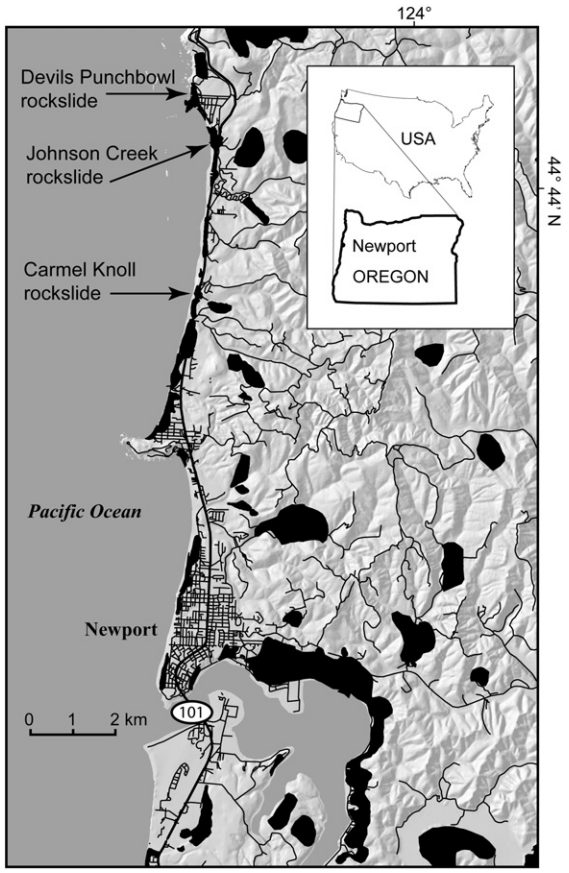

Fig. 1. Map showing location of study. Landslides mapped previously (Burns et al., 2011) are in black and the rockslides evaluated during this study are noted. Black lines indicate roadways.

Uplift of the rock and terrace sands and action of ocean waves has resulted in formation of bluffs typically 35–45 m high. In the three rockslide areas, bluffs retreat at rates of 0.15–0.24 m/y (Priest and Allan, 2004). The bluffs are sloped ~60°–90° where they are presently stable. However, landslides are pervasive (e.g., Schlicker et al., 1973; Gentile, 1978). Nearly all bluffs are fronted by persistent shallow landslides (few meters thick). Much larger rockslides and rockslide deposits that extend as much as hundreds of meters landward occur sporadically (Fig. 1). These are thick (tens of meters) with gently sloping basal failure surfaces occurring in the sedimentary bedrock near and below sea level. Landslides and landslide deposits also are widespread in the nearby Coast Range mountains. Priest and Allan (2004) identified 216 landslides primarily along the shoreline in northern Lincoln County (location of our study) and Burns et al. (2011) mapped the boundaries of 773 landslides in the entire county; these landslides cover 12.2% of its area. Additionally, Burns et al. (2011) documented the locations of 889 historical landslides in the county; an unknown number of these correlate with the 773 landslides whose boundaries were mapped.

Landslide activity is most extensive during the rainy months of October–March (North and Byrne, 1965; Schlicker et al., 1973) when about 78% of the 1.72 m of annual rainfall occurs (based on records from 1893 to 2010 for Newport weather station 356032; WRCC, 2011). Infiltration of rainwater results in elevated pore-water pressures that reduce effective stresses and, consequently, frictional strength of slope materials, which results in landslide reactivation. The large, seasonally active rockslides that occur in the sedimentary rock units typically move a few centimeters to a few decimeters each year. Many of these seasonally active rockslides are smaller reactivations of much larger but presently dormant rockslides (Gentile, 1978; Priest and Allan, 2004). Historical formation of the large rockslides outside of larger dormant rockslides is apparently very rare, and the ages of the rockslides we studied are unknown. However, U.S. Highway 101 has been damaged by movement of the Carmel Knoll and Johnson Creek rockslides since its construction during the 1940s (Oregon Department of Transportation and Geotechnical Group, 1986; Priest et al., 2006); thus these rockslides formed prior to highway completion during 1943. The apparent prehistoric formation of so many large rockslides and their large total displacements (tens of meters) relative to small annual displacements caused some to surmise that they were formed during a wetter climatic cycle or during earthquake ground shaking (Komar, 2004; Priest and Allan, 2004). Several studies have found that regional climatic conditions have been steady for at least the past 600 years (Keen, 1937; Graumlich, 1987; Worona and Whitlock, 1995; Gedalof and Smith, 2001). Most relevant to the present study, Graumlich (1987) estimated annual precipitation for the region for the 300-year period

of 1675–1975 using tree ring data and historical precipitation data. She found that the mean precipitation for this period was equivalent to the historical (1899–1975) mean. Based on Graumlich's reconstructed precipitation indices, one-year periods considered extremely wet (McKee et al., 1993) occurred about 1702, 1715, 1811, 1863, and 1969, while one-year periods considered extremely dry occurred about 1695, 1720, 1736, 1775, 1829, 1840, 1890, 1899, 1921, 1930, and 1970. From running 8-year averages, a period considered moderately wet occurred from 1700 to 1705 while periods considered moderately dry occurred from 1735 to 1737 and from 1929 to 1931; precipitation during all other periods was considered near normal.

3. Methods

We characterized the rockslides through field mapping, subsurface exploration, in situ monitoring of rockslide movement and hydrologic conditions, and analyses of results from previous studies. The Carmel Knoll and Johnson Creek rockslides are crossed by U.S. Highway 101 and have been periodically studied since the 1970s, providing a large amount of subsurface and laboratory data that were available for our use (ODOT Geotechnical Group, 1986; Landslide, 2004; Priest et al., 2006; Ellis et al., 2007; Schulz and Ellis, 2007; Kleutsch, 2008; Niem, 2008; Priest et al., 2011). To our knowledge, the Devils Punchbowl rockslide had not been studied previously; its impact is very limited as it occurs mostly within an undeveloped state park.

3.1. Surface and subsurface characterization

We mapped engineering geologic conditions onto topographic base maps created using total-station theodolites. Although the rockslides are densely vegetated, numerous geologic exposures exist along scarps, the coastal bluff, and within the tidal zone. To explore the subsurface, we bored holes through the head (upslope end) and toe (downslope end) of the Devils Punchbowl rockslide, four holes through the Johnson Creek rockslide, and hand excavated pits within the tidal zone to expose the bases of each rockslide. We evaluated logs from 71 holes at the Carmel Knoll rockslide and 13 holes at the Johnson Creek rockslide that were bored during previous investigations, monitoring records from 17 slope inclinometers at Carmel Knoll and 9 slope inclinometers at Johnson Creek (ODOT Geotechnical Group, 1986; Landslide, 2004; Kleutsch, 2008), and a structural cross section of the Johnson Creek rockslide (Niem, 2008). Bedding orientations provided supplemental information on rockslide subsurface geometry; varying degrees of bed rotation were used to interpret geometry of the basal rupture surfaces.

For use in our analyses of rockslide formation, we characterized rock-mass strength accounting for discontinuities as well as strength of intact rock. To do so, we utilized the Hoek–Brown failure criterion (Hoek et al., 2002) and results from six uniaxial compression tests of intact samples of the Astoria Formation (Cornforth Consultants, Inc., 2003; Shannon and Wilson, Inc. and Wilson, 2006), our observations of the rock mass in hundreds of meters of rock core and bluff exposures, and evaluation of more than 100 geological boring logs (ODOT Geotechnical Group, 1986; Cornforth Consultants, Inc., 2003; Landslide Technology, 2004; Shannon and Wilson, Inc., 2006; Bernard Kleutsch [ODOT], written communication, 2008). Zhao (2000) found that the Hoek–Brown criterion provides strength estimates that are well suited for dynamic analyses, and the criterion are widely used in engineering practice and research. For our analyses of rockslide reactivation, we estimated residual strength of the rockslide basal shear surfaces using limit-equilibrium modeling as described in Section 3.3.

3.2. Monitoring

Depths of landsliding and pore-water pressures were identified during previous investigations at the Carmel Knoll and Johnson Creek rockslides (ODOT Geotechnical Group, 1986; Landslide Technology, 2004; Kleutsch, 2008). We estimated the depth of the Devils Punchbowl rockslide from surface exposures and our two boreholes. At Carmel Knoll between January 2008 and June 2011, we continuously (5- to 15-min intervals) recorded slide movement from a cable extensometer (0.7 mm accuracy) we placed across the head of the rockslide and pore-water pressures from two piezometer arrays (0.3 kPa accuracy) located near the slide toe and head that remained from previous ODOT studies (Fig. 2). We installed piezometer arrays in our two boreholes at Devils Punchbowl and continuously monitored these between January 2008 and June 2011. An extensometer was installed to measure movement across the slide head during August 2009 and we monitored it continuously until June 2011. At Johnson Creek beginning in November 2004, we continuously monitored slide movement from three borehole extensometers and pore-water pressures from three piezometers installed during earlier studies (Fig. 2; Landslide Technology, 2004). Along with ODOT, we installed three piezometer arrays and two groundwater-monitoring wells at Johnson Creek (Fig. 2) during November 2006; we continuously monitored these and the preexisting sensors until June 2011.

3.3. Rockslide stability modeling

We followed several approaches to evaluate whether the rockslides were likely initiated by elevated pore-water pressures or earthquake-induced ground motion. To evaluate rockslide initiation and stability and basal strength of existing rockslides, we used the general limit equilibrium (GLE; Fredlund and Krahn, 1977; Fredlund et al., 1981) method-of-slices technique and a half-sine interslice force function; modeling was performed using the software Slide v.6 (Rocscience). The GLE is the most rigorous limit-equilibrium approach for analyzing stability of landslides with irregular basal geometry (e.g., Sharma, 2007). The method calculates force and moment equilibrium of slope cross sections divided into multiple vertical, two-dimensional slices while accounting for the interaction of each slice with its neighbors. The resulting ratios between stresses and moments resisting motion to those driving motion are used to estimate the factor of safety, which is greater than one for stable slopes, less than one for unstable slopes, and equal to one for slopes at the point of incipient failure.

3.3.1. Stability model development

To analyze initial formation of the rockslides, we estimated pre-rockslide topography (Fig. 3), which was straightforward considering the consistent, relatively flat, horizontal surface of the marine terrace along which the rockslides occur and considering the geometries of unfailed bluff profiles near the slides. To account for bluff retreat that has occurred since formation of the slides, we extended the bluff seaward so that its base intercepted the projection of the present-day location of the basal failure surface. Groundwater flow parallel to the water table was assumed for all analyses as this condition was indicated by monitoring observations (Schulz and Ellis, 2007; Schulz et al., 2009; Priest et al., 2011). We used the means of moist and saturated unit weights determined in the laboratory during previous studies (ODOT Geotechnical Group, 1986; Cornforth Consultants, Inc., 2003; Landslide Technology, 2004; Shannon and Wilson, Inc., 2006; Kleutsch, 2008) for the Astoria Formation (21.2 kN/m^3 and 25.5 kN/m^3, respectively) and marine terrace sand (18.3 kN/m^3 and 23.6 kN/m^3, respectively) during all analyses. For analyses involving reactivation of the existing rockslides, we estimated residual shear strength of the rockslide basal rupture surfaces

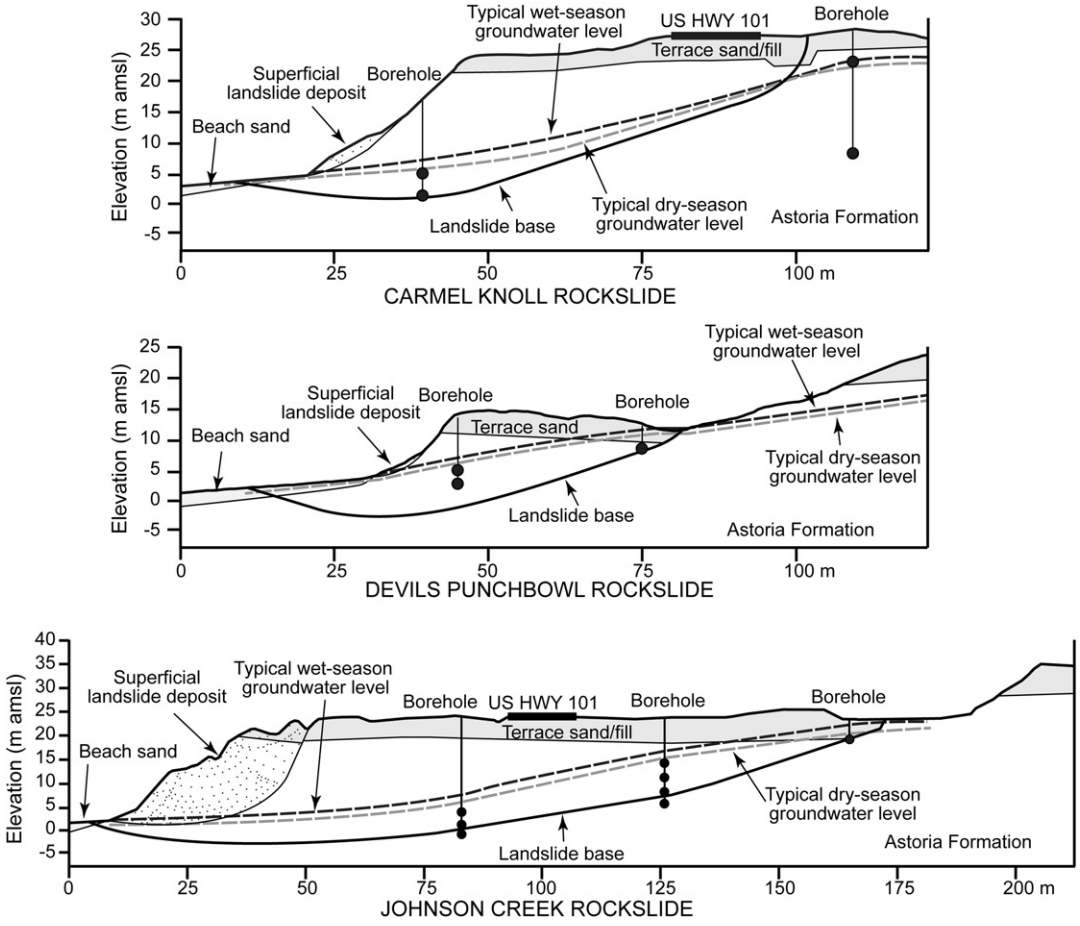

Fig. 2. Present-day geologic cross sections of the three rockslides. Piezometers monitored during this study are indicated by black circles. Means of observed dry-season (May–September) groundwater levels and observed levels at which movement is triggered during the wet season are shown. Geologic contacts are approximately located.

using groundwater conditions observed from monitoring at the onset of rockslide movement (factor of safety of 0.999). For analyses of initial formation of the rockslides, we used mean strength values for the terrace sand determined in the laboratory during previous studies (cohesionless, angle of internal friction of 32°; Landslide Technology, 2004; Shannon and Wilson, Inc., 2006; Kleutsch, 2008) and estimates of rock-mass strength of the Astoria Formation obtained as described in Section 3.1.

3.3.2. Gravitational stability — observed basal geometry

We evaluated gravitational stability for rockslide formation along observed basal rupture surfaces considering three different groundwater scenarios: (i) as observed recently during the dry season, (ii) as observed recently during the wet season, and (iii) an "extreme" scenario where the groundwater level was raised by as much as 30 m until it reached the ground surface (Fig. 3). We modeled the extreme groundwater scenario in order to consider the ultimate potential for elevated pore-water pressures to trigger formation of the landslides, although it is very unlikely that such groundwater conditions have been present during the past 600 years (Keen, 1937; Worona and Whitlock, 1995; Gedalof and Smith, 2001), and even less likely since the year 1675, as work by Graumlich (1987) suggests that groundwater conditions since 1675 were probably similar to the recently observed conditions.

3.3.3. Seismic stability — observed basal geometry

We evaluated seismic stability for rockslide formation along observed basal rupture surfaces by iteratively applying modeled seismic loads until the factor of safety for each scenario was 0.99, indicating formation of the rockslides. These evaluations provided the horizontal ground acceleration necessary to trigger slide movement, which is referred to as the yield acceleration (a_y). We considered dry- and wet-season groundwater conditions but did not evaluate a_y for the extreme groundwater scenario as all available evidence indicates that it is unrealistic. We also calculated factors of safety for rockslide formation considering peak horizontal ground accelerations of 1 and 2 g, where g is gravitational acceleration (9.807 m/s^2). These are reasonable estimates of ground acceleration for the geologic setting of the rockslides (see Section 3.4).

For our analyses of coseismic reactivation of the existing rockslides, we used cross sections of present-day rockslide geometries, residual strengths estimated from present-day reactivation conditions (Section 3.3.1), and observed dry-season groundwater conditions to estimate a_y needed to initiate movement of each rockslide during periods of low groundwater level. We did not analyze the a_y necessary during the winter rainy season as the rockslides are generally already moving during this time ($a_y = 0$).

During seismic stability analyses, constant earthquake accelerations were applied through the center of mass of each slice of the rockslides with a horizontal component directed toward the slope face (from east to west) and a vertical component directed either upward or downward during different iterations. We assumed that the vertical accelerations were two-thirds of the horizontal accelerations. An earthquake load results in deformation of soil and rock that occurs so rapidly that much of the load may be transferred to the pore water causing development of excess pore-water pressure that reduces the effective stress and frictional strength along surfaces of potential shearing. We accounted for this during seismic analyses by including

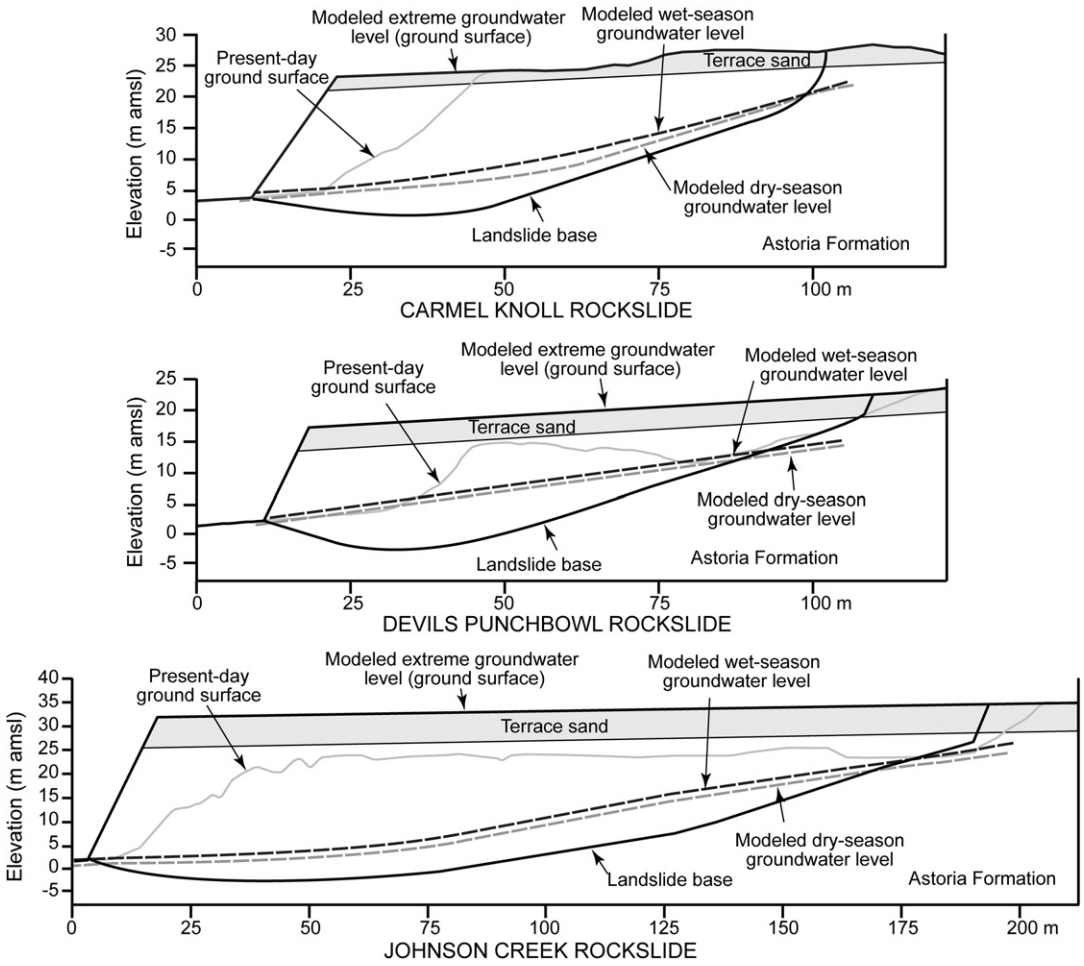

Fig. 3. Geologic cross sections of assumed conditions at the time of rockslide formation. Groundwater conditions represent means of observed dry-season (May–September) groundwater levels, observed levels at which movement is triggered during the wet season, and an extreme groundwater scenario where the level corresponds to the ground surface. Geologic contacts are approximately located.

generation of excess pore-water pressures from seismic loading and utilizing a Skempton B parameter equal to one, which is suitable for saturated soil and rock (Skempton, 1954).

3.3.4. Gravitational and seismic stability — variable basal geometry

As just described, the analyses of rockslide formation utilized the observed rockslide basal geometries. As a means of checking our results, we omitted the observed basal geometries and utilized algorithms to create 25,000 potential failure geometries whose stabilities were then analyzed for each stability scenario and assuming wet-season groundwater conditions. As the observed rockslide bases are primarily planar but include rotational components also (Fig. 2), we evaluated noncircular basal geometries. The algorithms for creating potential failure geometries are largely based on slope geometries. The bluffs have very low relief relative to the lengths of the rockslides so, to force creation of potential failure geometries ranging from very small (few meters long) to longer than those observed, we required that the potential failure surfaces be composed of line segments at least 12, 15, and 20 m long for the Carmel Knoll, Devils Punchbowl, and Johnson Creek slides, respectively; longer segment lengths were required for longer rockslides. We imposed no restrictions on potential locations of failure surface–ground surface intersections. The rock-mass strength estimates were used for all seismic analyses. Soft rock such as the Astoria Formation may suffer weakening over time through stress concentration and strain softening, which results in loss of cohesion (e.g., Martin, 1997; Hajiabdolmajid et al., 2002). Therefore, we evaluated gravitational stability while iteratively reducing cohesion until failure was indicated. During seismic analyses, we considered peak horizontal ground accelerations of 1 and 2 g, which are reasonable for the geologic setting of the rockslides (Section 3.4). We compared the observed failure geometries to the predicted least-stable geometries for each failure scenario.

3.4. Coseismic displacement modeling

The GLE method provides no information regarding what failure implies with respect to landslide displacement, only whether failure is expected. We therefore followed the Newmark approach, which is suitable for obtaining rapid estimates of the order of magnitude of seismically induced landslide movement (Newmark, 1965) and is most applicable for rigid landslide bodies whose downslope motion is restrained primarily by friction; thus it is well suited for the translational rockslides we studied. Previous studies of seismically triggered historical landslides on natural slopes have indicated the utility of the method, having generally predicted displacements of approximately 0.5–2 times those observed (Wilson and Keefer, 1983; Pradel et al., 2005). Simplifications of the method are used extensively to evaluate regional earthquake-induced landsliding (e.g., Rathje and Bray, 1999; Miles and Keefer, 2000; Romeo, 2000; Jibson, 2007). To estimate landslide displacement, Newmark's method involves doubly integrating that part of a horizontal seismic acceleration time history that exceeds the acceleration necessary to trigger landslide movement (a_y). We followed the method proposed by Wilson and Keefer (1983) to perform stepwise integration of the

acceleration record, while restricting potential slide motion to the downslope direction. Newmark and others (e.g., Franklin and Chang, 1977; Ambraseys and Menu, 1988; Jibson, 1993) believed this restriction to be reasonable because accelerations necessary for moving landslide blocks upslope can be extremely large. We used the estimates of a_y obtained during pseudostatic analyses for estimating Newmark displacements, as Newmark (1965) noted is most appropriate.

No large earthquakes have occurred along the Cascadia subduction zone since 1700; hence, no suitable earthquake acceleration time histories from the region exist for our displacement or stability analyses. Therefore, we used acceleration time histories recorded in Japan during the 11 March 2011, M 9.0 Tohoku earthquake, which occurred along the Japan Trench subduction zone (USGS, 2011) and triggered hundreds of landslides, including shallow and deep (to about 30 m) failures, some with extensive travel distances and catastrophic results (Sasahara et al., 2011; Gonghui Wang, Kyoto University, personal communication, 2011). We identified two seismic monitoring stations in Japan of the Kyoshin Network (K-NET) that have similar geological characteristics to those present at the Oregon rockslides. The time histories from this network are freely available (K-NET, 2011). Station MYG012 is located about 118 km from the 11 March 2011 epicenter and situated upon early Miocene conglomerate, sandstone, and siltstone (Takizawa et al., 1992) with $V_s = 880$ m/s. Station IWT010 is located about 129 km from the 11 March 2011 epicenter and situated upon middle Miocene siltstone and sandstone (Takizawa et al., 1992) with $V_s = 730$ m/s. These two stations recorded peak horizontal ground accelerations during the Tohoku earthquake of 2 and 1 g, respectively. Although the distances between the Japanese stations and Tohoku epicenter (~118 and 129 km) are greater than that between the rockslides and the Cascadia trench (~90 km), sufficient uncertainty exists in the location of a future Cascadia earthquake and in site-response effects that we believed it was inappropriate to scale the Japan records for our use. Each acceleration time history we used consists of east–west, north–south, and vertical components. Because of the opposite sense of subduction between the Japan Trench and Cascadia subduction zones, we reversed the east–west records and then calculated the horizontal accelerations parallel to the rockslide movement azimuths for use during our displacement analyses.

4. Results

4.1. Rockslide geometry and composition

The rockslides are 200–360 m wide, 100–200 m long, and have maximum thickness of 16–27 m (Fig. 2). Each slide encompasses a relatively small area of the tidal zone, the bluff, and a relatively large area of the marine terrace. Ground fractures in the marine terrace are extensive parallel to and within a few tens of meters of the bluff crest; these fractures mark the heads of superficial landslides that occur in most places along the bluffs. A graben as much as ~20 m across and ~7 m deep exists along parts of each rockslide head. Deformation of the ground surface located between the grabens and superficial landslides is largely absent suggesting block-like movement of the rockslides since their formation. Repeat monitoring of survey monuments spread across the surface of the Johnson Creek rockslide also suggests block-like movement (Priest et al., 2006). Movement of all three slides is translational along most of their lengths with rotation occurring in the toe region of each.

United States Highway 101 is aligned along the head of the Carmel Knoll rockslide so it has been modified by grading associated with road construction and maintenance, mainly involving filling of the graben formed at the slide head. The highway was located immediately east (to the right) of the location shown in Fig. 2 until it was rerouted during the 1990s. The Devils Punchbowl rockslide is essentially unmodified. Grading during construction and maintenance of the Old Coast Highway (predecessor of U.S. Highway 101) also modified some of the head of the Johnson Creek rockslide. This alignment was abandoned during the 1940s (Priest et al., 2006) following construction of U.S. Highway 101, which is aligned along the central part of the rockslide. The slides are nearly entirely comprised of Astoria Formation siltstone, although the unit is sandier at Devils Punchbowl and some sandstone beds occur there. Marine terrace sand 2–5 m thick caps the rock at each of the slides. Superficial landsliding is extensive at Johnson Creek, with shallow landslides extending as far as 40 m back from the bluff face; whereas superficial landslides are more limited in extent at Carmel Knoll and Devils Punchbowl. Minor colluvium occurs within grabens at the head of each slide.

Bedding within the Astoria Formation is difficult to discern except at the Devils Punchbowl rockslide because much of the unit is massive and facies variations are subtle. In some areas, the basal rupture surfaces are subparallel to bedding so may locally follow weaker beds or bedding planes. However, relatively weaker beds or bedding planes were rarely discernible in outcrop or core samples. Furthermore, rupture surfaces in the slide toe regions extend across ~5 m of bedding, and we observed no failures along the bluffs that occur along bedding planes that daylight through the bluff faces; these observations suggest that bedding has little control on the occurrence and geometry of the rockslides. Immediately outside of the slides, beds generally strike nearly north–south and dip to the west at 13–28°. Bedding attitudes are similar within the slides except within rotated toe regions. Fracturing is pervasive within the rockslides and less extensive outside of them. Dominant fracture systems are subvertical and strike ~N70W and ~N45E. Outside of the slides, these fractures are spaced 5–10 m, are generally tightly closed, and typically are coated by oxidized clay ~1–5 mm thick, occasionally with slickensides. Fracturing within the slides is spaced 0.3 to 3 m, and local crushed zones also occur. Borehole samples revealed clay-coated, occasionally slickensided fractures with 30–60° dips with average spacing of ~7 m. Core was not oriented, hence strikes of these fractures are unknown. Our observations, the average unconfined compressive strength of intact rock specimens (2.75 MPa), and the Hoek–Brown failure criterion (Hoek et al., 2002) indicate cohesion of 112 kPa and an internal friction angle of 26.7° for the rock-mass strength of the Astoria Formation outside of the rockslides.

The basal rupture surfaces of the slides exposed in the tidal zone consist of 20–100 mm of pulverized rock within which are 1–20 mm-thick, clayey, occasionally striated, tabular lenses. Similar descriptions of the basal ruptures at Carmel Knoll and Johnson Creek are found on lithological boring logs. Laboratory tests indicate that the basal ruptures consist of highly plastic (CH per ASTM D 4318, ASTM International, 2008), clayey silt (per ASTM D422, ASTM International, 2008).

4.2. Monitoring observations

Monitoring and visual observations indicated that the groundwater table was near the ground surface at the head of each rockslide and again at beach level. Within much of the slide bodies, groundwater occurs at average depths of about 14, 6, and 17 m for Carmel Knoll, Devils Punchbowl, and Johnson Creek, respectively (Fig. 2). These depths varied generally within 2 m but by as much as 6 m between the lowest dry-season levels and highest wet-season levels (Fig. 4). Piezometer arrays indicate that groundwater flow was subparallel to the water table. During our study (November 2002–June 2011), annual rainfall measured in Newport (station 356032) for water years beginning July 1 and ending June 30 was 78–92% of the annual average for the period 1893–2011 (WRCC, 2011).

Rockslide movement occurred during each rainy season and each episode was short lived, lasting hours to a few days. During each of

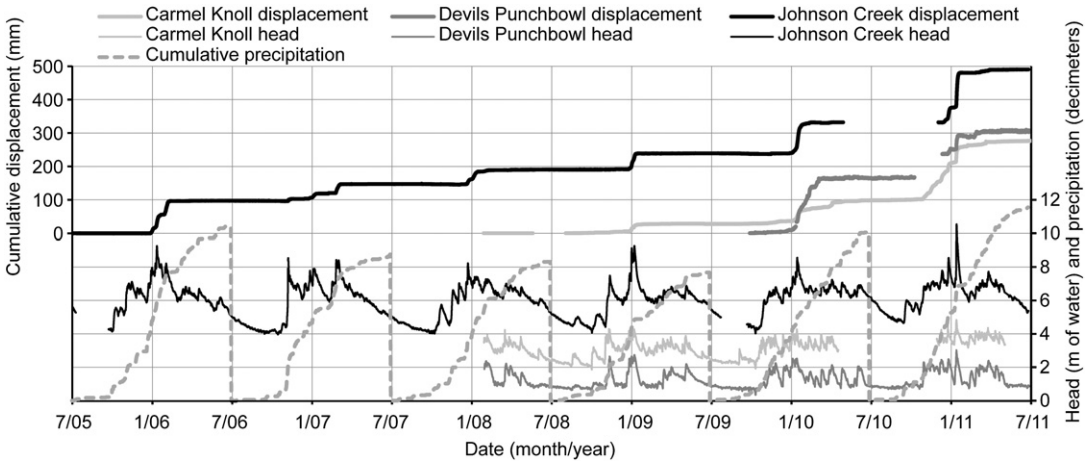

Fig. 4. Results from continuous monitoring from 1 July 2005 to 30 June 2011. Cumulative rainfall (NMA, 2011) is calculated between 1 July and 30 June. Carmel Knoll and Devils Punchbowl head data are from the deepest piezometers located near the rockslide toes (Fig. 2). Johnson Creek data are from the center monitoring site with head measurements from the piezometer located nearest to and above the basal rupture surface (Fig. 2). Most monitoring commenced at Carmel Knoll and Devils Punchbowl during January 2008; however, displacement monitoring commenced at Devils Punchbowl during August 2009. Head values were offset to arbitrary datums for clarity. Data gaps exist because of equipment failures.

the 13 movement events observed at Johnson Creek, movement commenced within minutes to a few hours at each of the three extensometers located along the longitudinal axis of the slide, suggesting that the slide moves as a semi-coherent block. At the other 2 rockslides, observations of fracture opening, movement along bounding faults, and at extensometers suggest the same block-like movement. Movement events commenced when specific pore-water pressure levels were exceeded following periods of intense rainfall; at each rockslide at least one piezometer indicated standard deviations of <0.5 m for pore-water pressure heads at which all movement episodes commenced, implying that pore-water pressure increase is primarily responsible for observed reactivation of the slides. These threshold pressure heads were within 2 m of dry-season low pressures. The three monitoring locations at the Johnson Creek rockslide indicated average annual displacement of 63–91 mm during the 2002–2011 wet seasons (2002–2004 records from Priest et al., 2006). The head of the Carmel Knoll rockslide had average annual displacement of 92 mm during the three wet seasons of 2008–2011, while the head of the Devils Punchbowl rockslide had average annual displacement of 152 mm during the two wet seasons of 2009–2011. Variability in annual movement was significant; Table 1 provides movement records for each year. The variability in annual movement somewhat correlates with total annual rainfall (Table 1) but correlates better with the abundance of generally short-lived (hours to few days), intense rainfall events (Fig. 4; Schulz et al., 2009; Priest et al., 2011). Although erosion of the rockslide toes by wave action also renders the slides more prone to movement, attempts to correlate movement with erosion have been unsuccessful (e.g., Priest et al., 2006).

4.3. Rockslide initiation modeling

Stability modeling suggests that the rockslides could not have formed from gravitational loading and rising pore-water pressures, even considering the scenario of extreme groundwater level; however, reasonable seismic loads during dry or wet seasons would trigger formation of the rockslides. Table 2 provides analysis results considering the observed rockslide failure geometries and Table 3 provides results considering variable rockslide geometries. A factor of safety below 1 indicates failure.

4.3.1. Gravitational stability — observed basal geometry

The lowest factor of safety obtained during analyses of gravitational loading of the observed rockslide geometries was 3.29; for realistic wet-season groundwater conditions, the lowest value was 4.35 (Table 2). We performed a sensitivity analysis to evaluate what effects our rock-mass strength estimate had on the results. Analyses using cohesion and an angle of internal friction that were 70% of our best estimates provided minimum factors of safety of 2.25 for the extreme groundwater scenario and 2.97 for modeled wet-season groundwater pressures.

4.3.2. Gravitational stability — variable basal geometry

Analyses of 25,000 potential basal geometries for each rockslide modeled with gravitational loads, wet-season groundwater conditions, and cohesion reduction for the Astoria Formation indicated failure at cohesion values of 26.8, 16.3, and 44.5 kPa for Carmel Knoll, Devils Punchbowl, and Johnson Creek, respectively (Table 3). The predicted failures were very short (~5–12 m thick) and located along the bluff face (Fig. 5). The longer failure at Johnson Creek compared to the other two locations is likely due to the presence of thicker, cohesionless terrace sand at Johnson Creek. With the reduced cohesion values for the Astoria Formation, the factors of safety for the observed rockslide geometries were 2.93, 3.52, and 4.95 for Carmel Knoll, Devils Punchbowl, and Johnson Creek, respectively (Table 3).

Table 1
Results from rockslide displacement monitoring.

Water year[a]	Recorded movement (mm)			Cumulative rainfall (mm)
	Johnson Creek (center site)	Devils Punchbowl	Carmel Knoll	
2002	270			878
2003	20			827
2004	20			789
2005	95			1040
2006	50			876
2007	41			832
2008	48		28	767
2009	76	167	70	1005
2010	160	137	177	1155
Total	780	304	275	8169
Average	87	152	92	908
Standard deviation	81	21	77	130

[a] Year indicated begins July 1 of that year and ends June 30 of the following year; rainfall totals are from NMA (2011).

Table 2
Results from slope-stability modeling of rockslide formation with observed geometries[a].

Rockslide	Factor of safety						
	Gravitational loading			Seismic loading			
	Dry	Wet	Extreme	1 g, Dry	2 g, Dry	1 g, Wet	2 g, Wet
Carmel Knoll	4.44	4.35	3.29	0.68	0.41	0.66	0.40
Devils Punchbowl	5.27	5.18	3.89	0.77	0.48	0.75	0.47
Johnson Creek	6.38	6.29	4.60	0.60	0.35	0.58	0.34

[a] g = gravitational acceleration, 9.807 m/s^2; dry, wet, and extreme indicate modeled groundwater scenario.

4.3.3. Seismic stability — observed basal geometry

Considering our best estimates of rock-mass strength and the observed basal rupture surfaces, stability analyses including seismic loading suggested that peak horizontal ground accelerations of 0.58, 0.64, and 0.48 g would trigger initial failure of the Carmel Knoll, Devils Punchbowl, and Johnson Creek rockslides, respectively, during wet and dry seasons. These acceleration values are less than the peak horizontal ground accelerations recorded at the IWT010 and MYG012 stations during the M 9.0 Tohoku earthquake, which were 1 and 2 g, respectively. Factors of safety determined using estimated rock-mass strengths, observed rupture surfaces, wet- and dry-season groundwater conditions, and peak horizontal and vertical accelerations from these two stations were 0.34–0.77 (Table 2).

4.3.4. Seismic stability — variable basal geometry

Analyses of 25,000 potential geometries for each rockslide considering our best estimates of rock-mass strength, the peak ground accelerations recorded by the K-NET stations, and wet-season groundwater conditions indicated the least-stable geometries shown in Fig. 5. With the exception of the Johnson Creek slide subjected to a horizontal seismic acceleration of 1 g, the predicted least-stable geometries are quite similar to the observed rockslide geometries (Fig. 5) and factors of safety indicate failure in all cases (0.32–0.63, Table 3). The least-stable geometry under a 1 g horizontal seismic load predicted for Johnson Creek (factor of safety = 0.55) is relatively short (Fig. 5), while a geometry similar to that observed had a slightly greater factor of safety (0.57). The shorter predicted failure here is likely due to the presence of thicker, cohesionless terrace sand than at the other two slides.

To summarize the model analyses of potential initiation of the rockslides, the observed rockslide geometries are predicted to be very stable under gravitational loading and modeled groundwater conditions similar to those observed (factors of safety >4.3), even considering rock weakening with time (factors of safety >2.9). The observed geometries are predicted to be very unstable under reasonable seismic loads (factors of safety <0.7). Furthermore, analyses of 25,000 potential failure geometries ranging from very short (few meters long) to longer than those observed indicates that predicted least-stable geometries under seismic loads are very similar to the observed rockslide geometries (Fig. 5). Rock weakening with time under gravitational loads is predicted to cause small failures similar to the superficial failures observed upon the rockslides.

4.4. Coseismic displacement modeling

Assuming that the rockslides were initiated during the wet season by earthquake-induced ground shaking similar to that recorded by the IWT010 and MYG012 stations, the Newmark displacement analyses suggest that rockslide movement during formation would have been 1–5 mm using the IWT010 record and 2–5 cm using the MYG012 record.

As estimated from stability analyses, the present-day rockslide basal rupture surfaces have residual angles of internal friction of 15.8°, 13.4°, and 7.0° for Carmel Knoll, Devils Punchbowl, and Johnson Creek, respectively. Using these strengths and observed dry-season groundwater conditions, modeling indicated yield accelerations necessary to reactivate the rockslides of 0.002–0.007 g. These values are very low, which is indicative of the tenuous state of stability for the slides. Assuming that a future earthquake during the dry season produces ground motion similar to that recorded at the K-NET stations while the rockslide geometries are similar to present day, the displacement analyses suggest movement of 7–13 m using the IWT010 record and 10–17 m using the MYG012 record. Coseismic displacements during the wet season when the slides are already moving would be much greater. These estimates do not account for site-response effects on ground shaking and changing rockslide geometry, material properties, or pore-water pressures during movement, so they should not be considered absolute predictions of expected displacement. Rather, the predicted displacements suggest that the rockslides may experience at least several meters of displacement if the assumptions considered in the analyses are valid.

5. Discussion

Many factors are responsible for rockslide formation and movement along the Oregon coast. Of course, rockslides occur along the flat marine terrace because of tectonic uplift and wave erosion, which are responsible for forming the bluffs. Downcutting through the terrace by rivers and streams results in similar topography subject to landsliding. Our analyses indicate that gravitationally induced stresses are focused near to the bluff face, resulting in formation of the ubiquitous shallow landslides that persistently move soil and rock from the bluffs to the tidal zone. Formation of these failures may be assisted by progressive loss of cohesive strength and increased pore-water pressures during the wet season. Nevertheless,

Table 3
Results from slope-stability modeling of rockslide formation with observed and least-stable geometries considering wet-season groundwater conditions[a].

Loading condition	Factor of safety			
	Geometry			
	Least stable, gravity load	Least stable, 1 g load	Least stable, 2 g load	Observed
Carmel Knoll, gravity, cohesion reduction	**0.99**	2.83	2.96	2.93
Carmel Knoll, 1 g	0.85	**0.58**	0.60	0.66
Carmel Knoll, 2 g	0.55	0.37	**0.34**	0.40
Devils Punchbowl, gravity, cohesion reduction	**0.99**	3.43	4.00	3.52
Devils Punchbowl, 1 g	1.20	**0.63**	0.63	0.75
Devils Punchbowl, 2 g	0.56	0.36	**0.34**	0.47
Johnson Creek, gravity, cohesion reduction	**0.99**	5.75	4.37	4.95
Johnson Creek, 1 g	0.57	**0.55, 0.57**[b]	0.58	0.58
Johnson Creek, 2 g	0.36	0.33	**0.32**	0.34

[a] g = gravitational acceleration, 9.807 m/s^2; values for least-stable geometries for each loading condition are shown in bold.
[b] For Johnson Creek 1 g load scenario, factors of safety of 0.55 and 0.57 are for least-stable shallow and deep geometries (Fig. 5), respectively.

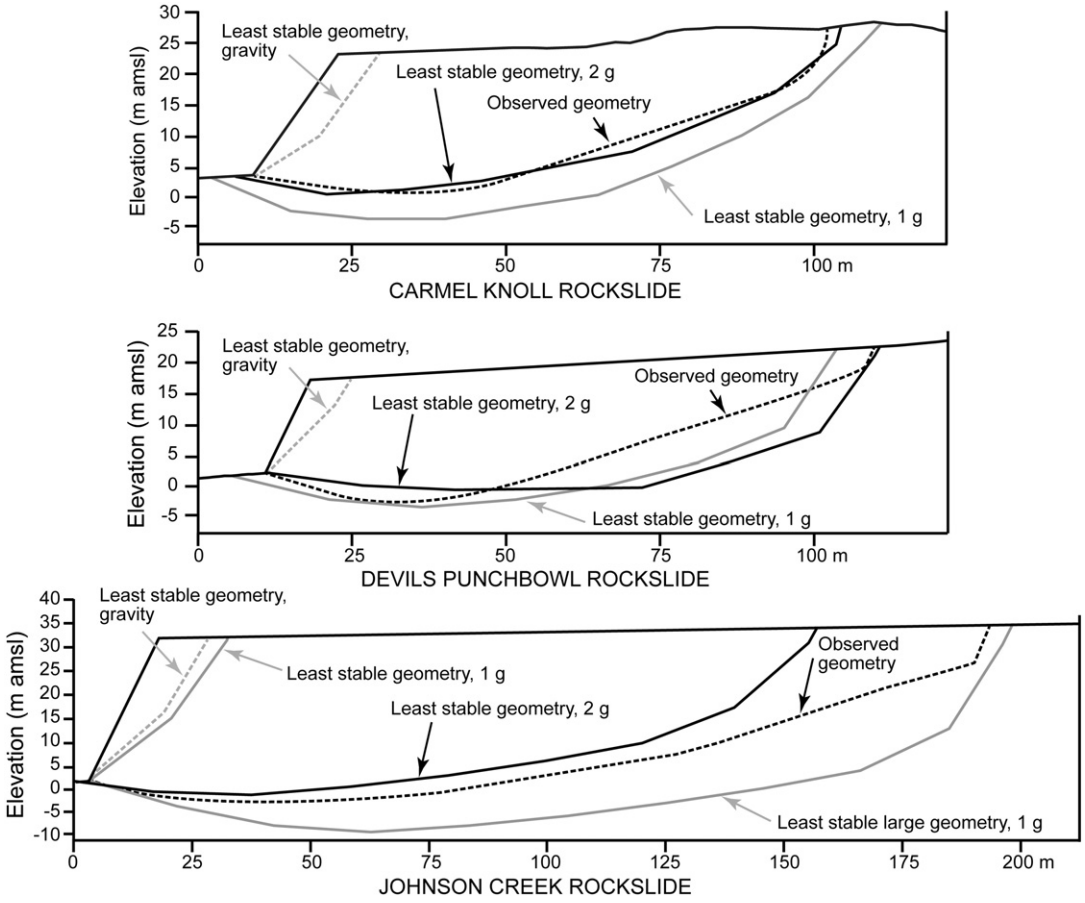

Fig. 5. Slope-stability modeling results. Least-stable rockslide geometries are depicted from gravitational and seismic loading analyses for wet-season conditions. 1 g and 2 g indicate peak horizontal ground accelerations used during seismic analyses. For 1 g loading at Johnson Creek, the least-stable geometry is shallow (factor of safety = 0.55) but a similarly unstable (factor of safety = 0.57) large geometry similar to the observed rockslide was identified also; both are shown.

gravitational loading alone appears to be unable to form the large, deep, translational rockslides that are also ubiquitous along the coast. Our analyses suggest that rockslides such as these form from ground motion accompanying Cascadia subduction-zone earthquakes. They may also form from ground motion accompanying earthquakes on other tectonic faults, but such earthquakes are unknown historically and we did not evaluate their potential effects. Rockslide geometries predicted to be least stable during seismic loading are similar to those observed, but not identical. The differences between predicted least-stable and observed geometries are due to many factors, likely including heterogeneity of the rock mass, differences between seismic loads that triggered the rockslides and those we used during modeling, and errors in our estimates of slope geometries, groundwater conditions, and rock-mass strength.

Measurements of total movement and recent annual movement permit the ages of the Devils Punchbowl and Johnson Creek rockslides to be estimated. For the Carmel Knoll rockslide, we have no data indicative of total movement, such as offset of stratigraphic markers or the ground surface, which has been extensively modified during roadway construction and maintenance activities. The age estimates are subject to a great deal of uncertainty because ground shaking from undocumented earthquakes and changes in rockslide geometries, material properties, pore-water pressures, wave erosion, and other conditions have likely affected rockslide movement since they formed. In addition, our monitoring records are very limited in time, and displacement during potential coseismic initiation of the slides is unknown. We were unable to obtain soils with which to perform radiometric dating; hence, our means of dating the slides were very limited.

A geological cross section based on detailed evaluations of borehole samples and surface exposures indicates that the Johnson Creek rockslide had moved a total of 28.6 m in the vicinity of the central extensometer by January 2003. Continuous monitoring indicated this location moved an additional 510 mm prior to June 2011, and monitoring for nine years indicated an average speed of 87 mm/y. This rate and the total displacement suggest that the Johnson Creek rockslide was 336 years old during 2011. Considering ± one standard deviation of the rate (Table 1), the estimated age range is 173 to 5510 years. The relative lack of human activity at the Devils Punchbowl rockslide permits estimating total rockslide displacement from offset of the ground surface. Our topographic survey indicates that the rockslide head moved a total of about 45 m. Continuous monitoring during water years 2009 and 2010 indicates that the head moved at an average speed of 152 mm/y. This rate and the total displacement suggest that the Devils Punchbowl rockslide was 296 years old during 2011. Considering ± one standard deviation of the rate (Table 1), the estimated age range is 260 to 344 years. Ignoring the great deal of uncertainty in the age estimates, the best estimates of 336 and 296 years, the relative stability of climatological conditions during the past 600 years, and the occurrence of an M 9.0 earthquake along the Cascadia subduction zone 311 years before the end of our monitoring suggest that formation of the rockslides was triggered by the earthquake.

Modeling and monitoring results support the conclusion that the rockslides were triggered by the M 9.0 Cascadia subduction-zone earthquake that occurred during January 1700. Stability and displacement analyses suggest that such an earthquake may trigger formation of large, deep rockslides but they will not move very far (a few

centimeters). Their formation will involve a significant decrease in strength as basal rupture surfaces propagate through the rock mass, which will render the rockslides susceptible to movement from increased pore-water pressures during the wet season and from erosion by wave action of rockslide toes; such erosion will be exacerbated along the bluffs as each Cascadia earthquake has involved coastal subsidence of about a meter (e.g., Nelson et al., 1995; Kelsey et al., 2002). Although newly formed deep rockslides may not move very far upon initiation, a great Cascadia earthquake will reactivate many large rockslides, even during the dry season, and many will move at least several meters. In addition to the large rockslides, our analyses suggest that earthquake ground motion will trigger many shallow failures along the bluffs, and the low yield accelerations for these failures and existing shallow slides suggest that they also will move distances of several meters.

Our findings indicate an interesting cycle of widespread rockslide triggering from a Cascadia earthquake with many new failures formed and many existing rockslides reactivated. Large reactivated slides and new shallow slides may move significant distances into the tidal zone, creating a large sediment influx that will be immediately susceptible to wave attack enhanced by coseismic coastal subsidence. Much of this rockslide debris in the tidal zone will likely be eroded by wave action in the few years to decades following the earthquake; while many of the newly formed, large, deep rockslides will commence their slow march toward the sea during wet seasons. The cycle will apparently repeat every 300–500 years, based on current understanding of recurrence of great Cascadia earthquakes.

The hazard to human safety presented by future earthquake-triggered reactivation of existing rockslides is likely to be significant. Reactivated deep rockslides and newly formed shallow landslides will likely render parts of U.S. Highway 101 and other roadways unusable, which may have disastrous effects on tsunami evacuation and emergency response activities. Future studies could be directed toward identifying and characterizing existing rockslides and areas susceptible to new rockslides along critical roadways and other infrastructure, especially with respect to potential coseismic displacement. Such studies would likely be of great benefit for hazard mitigation efforts.

6. Conclusion

Large, deep rockslides in Tertiary sedimentary rock are widespread along the Oregon coast. Many are dormant while many others experience renewed movement of a few centimeters during wet seasons, whereas their apparent total displacements suggest they are quite old. The Cascadia subduction zone located about 90 km offshore produces great earthquakes every 300–500 years; the last occurred during January 1700. We studied three typical large, deep rockslides to reveal mechanisms responsible for their formation. Monitoring for 2–9 years and measurements of total movement suggest that two of the rockslides are 296–336 years old; total movement of the third slide could not be determined. Limit-equilibrium slope-stability analyses suggest that the rockslides could not be formed by gravitational loading and increased pore-water pressures. Progressive strength loss, gravitational loading, and increased pore-water pressures likely trigger formation of the many shallow slides observed along the bluffs but are unlikely to trigger formation of the large rockslides. Stability analyses suggest that reasonable estimates of earthquake ground motion would trigger formation of the large rockslides. Estimates of coseismic displacement following the Newmark (1965) method suggest that, upon initiation, the rockslides would move only centimeters. However, upon reactivation during a subsequent earthquake, the rockslides would move several meters. Our findings clarify landsliding and geomorphic evolution of the dynamic coastal bluff environment of Oregon. Additionally, they suggest that tsunami evacuation and emergency response routes may be severed by landsliding during the next great Cascadia subduction-zone earthquake.

Acknowledgments

We are grateful to the following people and organizations for their assistance during this study: Bernard Kleutsch, Ed Duffy, and Katie Castelli with ODOT; George Priest and Jonathan Allan with DOGAMI; Claude Crocker and JR Collier with Oregon Parks & Recreation Department (OPRD); Gonghui Wang with Kyoto University; Rex Baum, Jeffrey Coe, William Ellis, Jonathan Godt, David Kibler, and Alan Nelson with the U.S. Geological Survey; and Joshua Theule, Brad Rickard, Alan Niem, and Wendy Niem. The Oregon Department of Transportation provided a wealth of background information on the Carmel Knoll and Johnson Creek rockslides, drilling services and monitoring equipment that we utilized at Johnson Creek, and access to both of these rockslides and previously installed monitoring equipment. The Oregon Parks & Recreation Department provided access to the Devils Punchbowl rockslide. Cornforth Consultants, Inc., Landslide Technology, and Shannon & Wilson, Inc. shared results from several geotechnical investigations. William Burns, William Haneberg, Jason Kean, and anonymous reviewers provided recommendations that improved this manuscript. Any use of trade, product, or firm names is for descriptive purposes only and does not imply endorsement by the U.S. Government.

References

Ambraseys, N.N., Menu, J.M., 1988. Earthquake-induced ground displacements. Earthquake Engineering and Structural Dynamics 16, 985–1006.
ASTM International, 2008. Annual Book of ASTM Standards, Volume 04.08, Soil and Rock (I). ASTM International, West Conshohocken, PA.
Atwater, B.F., Hemphill-Haley, E., 1997. Recurrence intervals for great earthquakes of the past 3,500 years at Northwestern Willapa Bay, Washington. U.S. Geological Survey Professional Paper, 1576. Reston, VA.
Burns, W.J., Mickelson, K.A., Saint-Pierr, E.C., 2011. SLIDO-2, Statewide Landslide Information Database for Oregon, Release 2. Oregon Department of Geology and Mineral Industries. . Portland, OR.
Clague, J.J., 1997. Evidence for large earthquakes at the Cascadia subduction zone. Reviews of Geophysics 35 (4), 439–460.
Cornforth Consultants, Inc., 2003. Depoe bay retaining wall landslide, geotechnical data report, phase 1 and phase 2, final addendum, Depoe Bay, Oregon. Technical report. . Portland, OR.
Ellis, W.L., Schulz, W.H., Priest, G.R., 2007. In: Schaefer, V.R., Schuster, R.L., Turner, A.K. (Eds.), Proceedings, 1st North American Landslide Conference, Vail, CO, 3–8 June 2007. AEG Special Publication No. 23. Association of Environmental & Engineering Geologists, Denver, CO, USA, pp. 921–934.
Franklin, A.G., Chang, F.K., 1977. Earthquake resistance of earth and rock-fill dams, report 5, permanent displacements of earth embankments by Newmark sliding block analysis. Miscellaneous Paper S-71-17, U.S. Army Engineer Waterways Experiment Station, Vicksburg, MS.
Fredlund, D.G., Krahn, J., 1977. Comparison of slope stability methods of analysis. Canadian Geotechnical Journal 14, 429–439.
Fredlund, D.G., Krahn, J., Pufahl, D.E., 1981. The relationship between limit equilibrium slope stability methods. Proceedings of the 10th International Conference on Soil Mechanics and Foundation Engineering, Stockholm, Sweden. A.A. Balkema, Rotterdam, Netherlands, pp. 409–416.
Gedalof, Z., Smith, D.J., 2001. Interdecadal climate variability and regime-scale shifts in Pacific North America. Geophysical Research Letters 28 (8), 1515–1518.
Geist, E.L., 2005. Local tsunami hazards in the Pacific Northwest from Cascadia subduction zone earthquakes. U.S. Geological Survey Professional Paper. 1661-B, Reston, VA.
Gentile, J.R., 1978. The delineation of landslides in the Lincoln County, Oregon coastal zone. MS Thesis, Oregon State University, Corvallis.
Goldfinger, C., Hans Nelson, C., Johnson, J.E., 2003. Holocene earthquake records from the Cascadia subduction zone and Northern San Andreas Fault based on precise dating of offshore turbidites. Annual Review of Earth and Planetary Sciences 31, 555–577.
Graumlich, L.J., 1987. Precipitation variation in the Pacific Northwest (1675–1975) as reconstructed from tree rings. Annals of the Association of American Geographers 77 (1), 19–29.
Hajiabdolmajid, V., Kaiser, P.K., Martin, C.D., 2002. Modelling brittle failure of rock. International Journal of Rock Mechanics & Mining Sciences 39, 731–741.
Heaton, T.H., Hartzell, S.H., 1987. Earthquake hazards on the Cascadia subduction zone. Science 236, 162–168.
Hoek, E., Carranza-Torres, C., Corkum, B., 2002. Hoek–Brown failure criterion — 2002 edition. In: Hammah, R. (Ed.), Proceedings of the NARMS-TAC Conference, Toronto. University of Toronto Press, Toronto, Ontario, Canada, Canada, pp. 267–273.

Jibson, R.W., 1993. Predicting earthquake-induced landslide displacements using Newmark's sliding block analysis. Earthquake-Induced Ground Failure Hazards, Transportation Research Record 1411. National Academy Press, Washington, D.C., USA, pp. 9–17.
Jibson, R.W., 2007. Regression models for estimating coseismic landslide displacement. Engineering Geology 91, 209–218.
Jibson, R.W., Keefer, D.K., 1993. Analysis of the seismic origin of landslides; examples from the New Madrid seismic zone. Geological Society of America Bulletin 105, 521–536.
Keen, F.P., 1937. Climatic cycles in eastern Oregon as indicated by tree rings. Monthly Weather Review 65 (5), 175–188.
Kelsey, H.M., Witter, R.C., Hemphill-Haley, E., 2002. Plate-boundary earthquakes and tsunamis of the past 5500 yr, Sixes River estuary, southern Oregon. Geological Society of America Bulletin 114 (3), 298–314.
Kelsey, H.M., Nelson, A.R., Hemphill-Haley, E., Witter, R.C., 2005. Tsunami history of an Oregon coastal lake reveals a 4600 yr record of great earthquakes on the Cascadia subduction zone. Geological Society of America Bulletin 117 (7/8), 1009–1032.
K-NET(Kyoshin Network), 2011. web site http://www.k-net.bosai.go.jp/2011Accessed 1 Sept. 2011.
Kleutsch, B., 2008, written communications.
Komar, P.D., 2004. Oregon's coastal cliffs: processes and erosion impacts. In: Hampton, M., Griggs, G. (Eds.), Formation, Evolution, and Stability of Coastal Cliffs, Status and Trends: U.S. Geological Survey Professional Paper, 1693, pp. 65–79. Reston, VA.
Landslide Technology, 2004. Geotechnical investigation, Johnson Creek landslide, Lincoln County, Oregon. Oregon Department of Geology and Mineral Industries Open File Report O-04-05. . Portland, OR.
Madin, I.P., Wang, Z., 1999. Relative earthquake hazard maps for selected coastal communities in Oregon. Oregon Department of Geology and Mineral Industries Interpretive Map Series IMS-10. . Portland, OR.
Martin, C.D., 1997. Seventeenth Canadian geotechnical colloquium: the effect of cohesion loss and stress path on brittle rock strength. Canadian Geotechnical Journal 34, 698–725.
McKee, T.B., Doesken, N.J., Kleist, J., 1993. The relationship of drought frequency and duration to time scales. Proceedings, Eighth Conference on Applied Climatology, Anaheim, CA, 17–22 January 1993. American Meteorological Society, Boston, MA, USA, pp. 179–184.
Miles, S.B., Keefer, D.K., 2000. Evaluation of seismic slope-performance models using a regional case study. Environmental & Engineering Geoscience vi (1), 25–39.
Nelson, A.R., Atwater, B.F., Bobrowsky, P.T., Bradley, L.A., Clague, J.J., Carver, G.A., Darienzo, M.E., Grant, W.C., Krueger, H.W., Sparks, R., Stafford Jr., T.W., Stuiver, M., 1995. Radiocarbon evidence for extensive plate-boundary rupture about 300 years ago at the Cascadia subduction zone. Nature 378, 371–374.
Nelson, A.R., Asquith, A.C., Grant, W.C., 2004. Great earthquakes and tsunamis of the past 2000 years at the Salmon River estuary, central Oregon coast, USA. Bulletin of the Seismological Society of America 94, 1276–1292.
Newmark, N.M., 1965. Effects of earthquakes on dams and embankments. Geotechnique 15 (2), 139–159.
Niem, A., 2008, written communications.
NMA (Newport Municipal Airport), 2011. website http://www.wunderground.com/history/airport/KONP/2005/7/1/DailyHistory.html?req_city=NA&req_state=NA&req_statename=NA2011accessed 21 Nov. 2011.
North, W.B., Byrne, J.V., 1965. Coastal landslides of northern Oregon. The Ore Bin 27 (11), 217–241.
ODOTOregon Department of Transportation, Geotechnical Group, 1986. Geotechnical investigation, slide stabilization, Carmel Knoll Slide, Oregon Coast Highway 9, M.P. 135, Lincoln County, C021-1424. Technical report. Salem, OR.
Pradel, D., Smith, P.M., Stewart, J.P., Raad, G., 2005. Case history of landslide movement during the Northridge earthquake. Journal of Geotechnical and Geoenvironmental Engineering 1360–1369 Nov.
Priest, G.R., 1995. Explanation of mapping methods and use of the tsunami hazard maps of the Oregon coast. Oregon Department of Geology and Mineral Industries Open-file Report O-95-67. Portland, OR.
Priest, G.R., Allan, J.C., 2004. Evaluation of coastal erosion hazard zones along Dune and Bluff backed shorelines in Lincoln County, Oregon: Cascade Head to Seal Rock. Oregon Department of Geology and Mineral Industries Open File Report O-04-09. Portland, OR.
Priest, G.R., Allan, J.C., Niem, A.R., Christie, S.R., Dickenson, S.E., 2006. Interim report: Johnson Creek landslide project, Lincoln County, Oregon. Oregon Department of Geology and Mineral Industries Open File Report O-06-02. Portland, OR.
Priest, G.R., Schulz, W.H., Ellis, W.L., Allan, J.A., Niem, A.R., Niem, W.A., 2011. Landslide stability: role of rainfall-induced, laterally propagating, pore-pressure waves. Environmental & Engineering Geoscience XVII (4), 315–335.
Rathje, E.M., Bray, J.D., 1999. An examination of simplified earthquake-induced displacement procedures for earth structures. Canadian Geotechnical Journal 36, 72–87.
Romeo, R., 2000. Seismically induced landslide displacements: a predictive model. Engineering Geology 58, 337–351.
Sasahara, K., Uchimura, T., Naka, S., Mukai, N., Yamabe, S., Yanagisaki, G., 2011. Landslides occurred by the 2011 off the Pacific coast of Tohoku earthquake in Fukushima Pref. and Tochighi, Pref. Journal of the Japan Society of Erosion Control Engineering 64 (2).
Satake, K., Shimazaki, K., Tsuji, Y., Ueda, K., 1996. Time and size of a giant earthquake in Cascadia inferred from Japanese tsunami records of January 1700. Nature 379, 246–249.
Schlicker, H.G., Deacon, R.J., Olcott, G.W., Beaulieu, J.D., 1973. Environmental geology of Lincoln County, Oregon. Oregon Department of Geology and Mineral Industries Bulletin, 81. Portland, OR.
Schulz, W.H., Ellis, W.L., 2007. Preliminary results of subsurface exploration and monitoring at the Johnson Creek landslide. Lincoln County, Oregon. U.S. Geological Survey Open-File Report 2007–1127, Reston, VA.
Schulz, W.H., Rickard, S.L., Higgins, J.D., 2009. Rapid response of deep bedrock landslides to rainfall, coastal Oregon. Geological Society of America Abstracts with Programs 41 (7), 378.
Shannon & Wilson, Inc., 2006. Geotechnical investigation, US 101: Spencer Creek Bridge, Lincoln County, Oregon. Technical report. . Portland, OR.
Sharma, S., 2007. Slope stability assessment using limit equilibrium methods. Landslides and Society In: Turner, A.K., Schuster, R.L. (Eds.), Proceedings of the First North American Conference on Landslides. Omnipress, Madison, WI, pp. 239–260.
Skempton, A.W., 1954. The pore pressure coefficients A and B. Geotechnique 4 (4), 143–147.
Takizawa, F., Yanagisawa, Y., Kubo, K., Kamada, K., 1992. Geological Map, Ishinomaki. Geological Survey of Japan, Tsukuba.
USGS (U.S. Geological Survey), 2011. web site http://earthquake.usgs.gov/earthquakes/eqinthenews/2011/usc0001xgp/2011accessed 1 Sept. 2011.
Wang, G., 2011, personal communication.
Wilson, R.C., Keefer, D.K., 1983. Dynamic analysis of a slope failure from the 6 August 1979 Coyote Lake, California, Earthquake. Bulletin of the Seismological Society of America 73 (3), 863–877.
Worona, M.A., Whitlock, C., 1995. Late Quaternary vegetation and climate history near Little Lake, Central Coast Range, Oregon. Geological Society of America Bulletin 107 (7), 867–876.
WRCC (Western Regional Climate Center), 2011. website http://www.wrcc.dri.edu/2011accessed 1 Sept. 2011.
Zhao, J., 2000. Applicability of the Mohr–Coulomb and Hoek–Brown strength criteria to the dynamic strength of brittle rock. International Journal of Rock Mechanics & Mining Sciences 37, 1115–1121.